Results and Discussion

1. Immobilization of lipase

The effect of enzyme loading on immobilization on Accurel was determined. The results are shown in Table 1. The hydrolytic activity of immobilized enzyme increased with increasing enzyme loading. On the other hand, the immobilized yield decreased with increasing the concentration of enzyme. These profiles could be due to limitation of substrate diffusion toward the surface and into the pore of the support because of its microporous nature. At high enzyme loading, steric hindrances caused by the excessive packing of the enzyme might occur. Moreover, the lipase molecules would penetrate and be immobilized to binding sites in the matrix pores, in sites inaccessible to the substrate. When the immobilized activity and immobilized yield were considered it was found that the concentration of enzyme with 50 U/mL was suitable for immobilized lipase PS on Accurel.

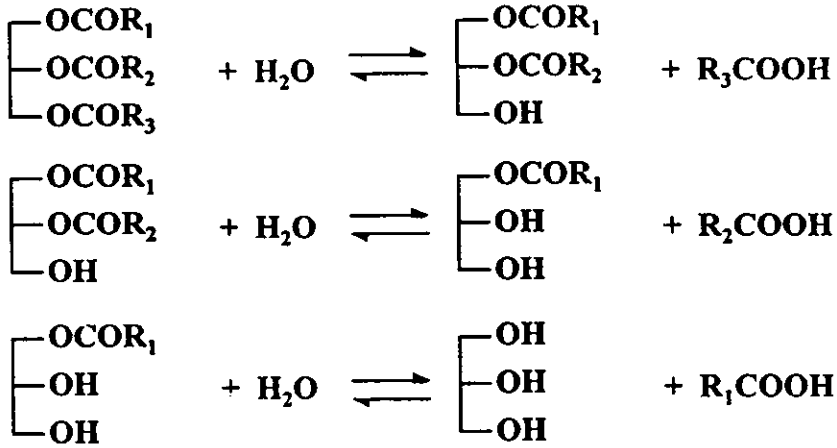Table 1 Effect of enzyme loading on immobilization of lipase PS with Accurel

Enzyme concentration U/mL	Immobilized yield (%)	Immobilized activity (U/mg support)
5	98.8[a]	0.14[a]
10	99.5[b]	0.18[b]
50	99.9[c]	0.33[c]
100	99.9[c, d]	0.34[c]
150	99.8[d]	0.45[d]

Different letters in the same column indicate significant differences ($p < 0.05$)

2. Modeling of lipase catalytic reaction

Mechanisms of lipase catalytic reactions based on hydrolysis, esterification and glycerolysis of triacylglycerol were considered. Starting with the reaction network shown in Figure 2, one can derive many rate expressions for the various cases in which different steps are taken as rate determining.

Hydrolysis and esterification

$$
\begin{bmatrix} -OCOR_1 \\ -OCOR_2 \\ -OCOR_3 \end{bmatrix} + H_2O \rightleftharpoons \begin{bmatrix} -OCOR_1 \\ -OCOR_2 \\ -OH \end{bmatrix} + R_3COOH
$$

$$
\begin{bmatrix} -OCOR_1 \\ -OCOR_2 \\ -OH \end{bmatrix} + H_2O \rightleftharpoons \begin{bmatrix} -OCOR_1 \\ -OH \\ -OH \end{bmatrix} + R_2COOH
$$

$$
\begin{bmatrix} -OCOR_1 \\ -OH \\ -OH \end{bmatrix} + H_2O \rightleftharpoons \begin{bmatrix} -OH \\ -OH \\ -OH \end{bmatrix} + R_1COOH
$$

Glycerolysis

$$
\begin{bmatrix} -OCOR_1 \\ -OCOR_2 \\ -OCOR_3 \end{bmatrix} + \begin{bmatrix} -OH \\ -OH \\ -OH \end{bmatrix} \rightleftharpoons \begin{bmatrix} -OCOR_1 \\ -OCOR_2 \\ -OH \end{bmatrix} + \begin{bmatrix} -OCOR_3 \\ -OH \\ -OH \end{bmatrix}
$$

$$
\begin{bmatrix} -OCOR_1 \\ -OCOR_2 \\ -OH \end{bmatrix} + \begin{bmatrix} -OH \\ -OH \\ -OH \end{bmatrix} \rightleftharpoons \begin{bmatrix} -OCOR_1 \\ -OH \\ -OH \end{bmatrix} + \begin{bmatrix} -OCOR_2 \\ -OH \\ -OH \end{bmatrix}
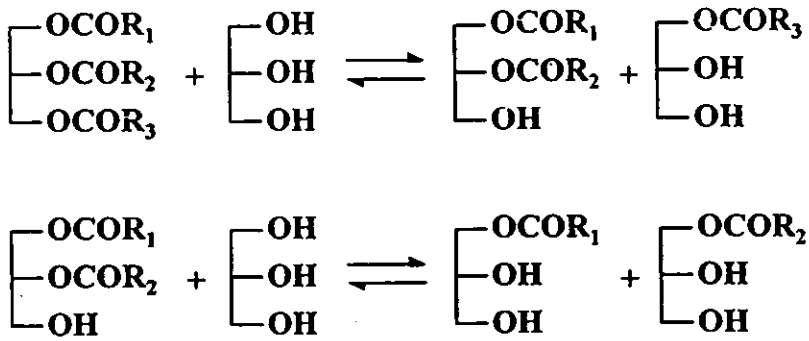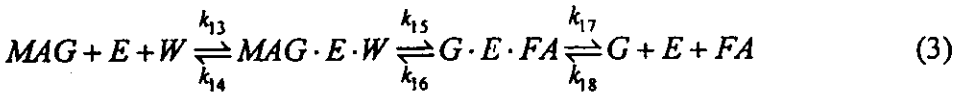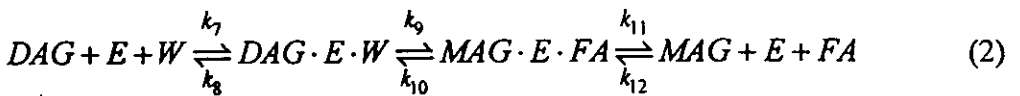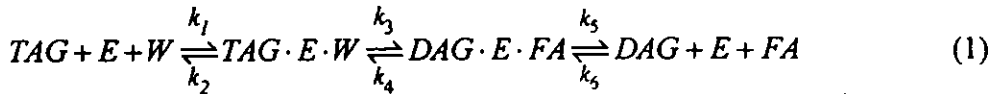$$

Figure 2 The main reactions of glycerolysis of palm olein (R: palmitin or olein).

All reactions for monoacylglycerol production were classed into two groups: one was hydrolysis and esterification group and another was glycerolysis group. Hydrolysis reaction for monoacylglycerol production was a stepwise of hydrolysis of triacylglycerol and diacylglycerol. Esterification reaction for monoacylglycerol production is a reverse reaction of hydrolysis of monoacylglycerol. Glycerolysis reaction for monoacylglycerol production was interesterification of tri- or di-acylglycerol with excess glycerol. The interesterification reaction involves sequential execution of the hydrolysis and reesterification steps, and thus requires multiple entrances and exits of reactant and product species in such a manner as to render the overall mechanism of the Ping-Pong type. It is important to emphasize that the hydrolysis step in glycerolysis reaction is the rate-determining step and then the reesterification of the released fatty acid to excess glycerol proceeds rapidly. Eventually glycerolysis reaction can be expressed by the initial reactants of tri- or di-acylglycerol and glycerol and products of two new acylglycerols as in Fig. 2. Glycerolysis of one mole triacylglycerol could produce 3 moles of monoacylglycerol, however monoacylglycerol yield depends on flavored equilibrium in various conditions. To describe a simple mathematical model for glycerolysis reaction, mass transfer limitation in reaction system was neglected. For modeling the data obtained at equilibrium, simple schemes of glycerolysis reaction shown by Equations (1-3).

$$TAG + E + W \underset{k_2}{\overset{k_1}{\rightleftharpoons}} TAG \cdot E \cdot W \underset{k_4}{\overset{k_3}{\rightleftharpoons}} DAG \cdot E \cdot FA \underset{k_6}{\overset{k_5}{\rightleftharpoons}} DAG + E + FA \tag{1}$$

$$DAG + E + W \underset{k_8}{\overset{k_7}{\rightleftharpoons}} DAG \cdot E \cdot W \underset{k_{10}}{\overset{k_9}{\rightleftharpoons}} MAG \cdot E \cdot FA \underset{k_{12}}{\overset{k_{11}}{\rightleftharpoons}} MAG + E + FA \tag{2}$$

$$MAG + E + W \underset{k_{14}}{\overset{k_{13}}{\rightleftharpoons}} MAG \cdot E \cdot W \underset{k_{16}}{\overset{k_{15}}{\rightleftharpoons}} G \cdot E \cdot FA \underset{k_{18}}{\overset{k_{17}}{\rightleftharpoons}} G + E + FA \tag{3}$$

The appearance rates of triacylglycerol (*TAG*), diacylglycerol (*DAG*), monoacylglycerol (*MAG*) and glycerol (*G*) from hydrolysis and reesterification steps were written as

$$\frac{d[TAG]}{dt} = -k_1[TAG][E][W] + k_2[TAG \cdot E \cdot W] \tag{4}$$

$$\frac{d[DAG]}{dt} = k_5[DAG \cdot E \cdot FA] - k_6[DAG][E][FA] - k_7[DAG][E][W] + k_8[DAG \cdot E \cdot W] \tag{5}$$

$$\frac{d[MAG]}{dt} = k_{11}[MAG \cdot E \cdot FA] - k_{12}[MAG][E][FA] - k_{13}[MAG][E][W] + k_{14}[MAG \cdot E \cdot W] \tag{6}$$

$$\frac{d[G]}{dt} = k_{17}[G \cdot E \cdot FA] - k_{18}[G][E][FA] \tag{7}$$

where W is water concentration, G is glycerol concentration, and E is free enzyme concentration. $TAG \cdot E \cdot W$, $DAG \cdot E \cdot FA$, $DAG \cdot E \cdot W$, $MAG \cdot E \cdot FA$, $MAG \cdot E \cdot W$ and $G \cdot E \cdot FA$ are different complexes between enzyme and the species defined above. The concentrations of the different enzymatic complexes can be expressed in terms of the free enzyme concentration by means of the following pseudoequilibrium relationships:

$$[TAG \cdot E \cdot W] = \frac{k_1}{k_2}[TAG][E][W] \tag{8}$$

$$[DAG \cdot E \cdot FA] = \frac{k_6}{k_5}[DAG][E][FA] \tag{9}$$

$$[DAG \cdot E \cdot W] = \frac{k_7}{k_8}[DAG][E][W] \tag{10}$$

$$[MAG \cdot E \cdot FA] = \frac{k_{12}}{k_{11}}[MAG][E][FA] \tag{11}$$

$$[MAG \cdot E \cdot W] = \frac{k_{13}}{k_{14}}[MAG][E][W] \tag{12}$$

$$[G \cdot E \cdot FA] = \frac{k_{18}}{k_{17}}[G][E][FA] \tag{13}$$

The total enzyme concentration (E_T) is given by

$$E_T = E + TAG \cdot E \cdot W + DAG \cdot E \cdot FA + DAG \cdot E \cdot W$$
$$+ MAG \cdot E \cdot FA + MAG \cdot E \cdot W + G \cdot E \cdot FA \tag{14}$$

By substitution of Eqs. (8-14) into Eqs. (4-7), and algebraic manipulation of the resulting equations, one obtains the following rate expressions:

$$\frac{d[TAG]}{dt} = \frac{(-V_{mDAG}[TAG][W] + V_{rDAG}[DAG][FA])E_T}{([W] + K_{mDAG}[DAG] + K_{mMAG}[MAG] + K_{mG}[G])[FA]} \tag{15}$$

where V_{mDAG} and V_{rDAG} are initial maximum reaction rates for hydrolysis of TAG (production of DAG) and reesterification of DAG defined as:

$$V_{mDAG} = \frac{k_1 k_3}{k_2} \text{ and } V_{rDAG} = \frac{k_4 k_6}{k_5}, \text{ respectively.}$$

K_{mDAG}, K_{mMAG} and K_{mG} are Michaelis constants for DAG, MAG and G defined as:

$$K_{mDAG} = \frac{k_1}{k_2}, \quad K_{mMAG} = \frac{k_7}{k_8} \text{ and } K_{mG} = \frac{k_{13}}{k_{14}}, \text{ respectively.}$$

$$\frac{d[DAG]}{dt} = \frac{(V_{mDAG}[TAG][W] + V_{rMAG}[MAG][FA] - V_{mMAG}[DAG][W] - V_{rDAG}[DAG][FA])E_T}{([W] + K_{mDAG}[DAG] + K_{mMAG}[MAG] + K_{mG}[G])[FA]} \quad (16)$$

where V_{mMAG} and V_{rMAG} are initial maximum reaction rates for hydrolysis of DAG (production of MAG) and reesterification of MAG defined as:

$$V_{mMAG} = \frac{k_7 k_9}{k_8} \text{ and } V_{rMAG} = \frac{k_{10} k_{12}}{k_{11}}, \text{ respectively.}$$

$$\frac{d[MAG]}{dt} = \frac{(V_{mMAG}[DAG][W] + V_{rG}[G][FA] - V_{mG}[MAG][W] - V_{rMAG}[MAG][FA])E_T}{([W] + K_{mDAG}[DAG] + K_{mMAG}[MAG] + K_{mG}[G])[FA]} \quad (17)$$

$$\frac{d[G]}{dt} = \frac{(V_{mG}[MAG][W] - V_{rG}[G][FA])E_T}{([W] + K_{mDAG}[DAG] + K_{mMAG}[MAG] + K_{mG}[G])[FA]}, \quad (18)$$

where V_{mG} and V_{rG} are initial maximum reaction rates for hydrolysis of MAG (production of G) and reesterification of G defined as:

$$V_{mG} = \frac{k_{13} k_{15}}{k_{14}} \text{ and } V_{rG} = \frac{k_{16} k_{18}}{k_{17}}, \text{ respectively.}$$

The formation and consumption of free fatty acid and water were derived from hydrolysis and esterification reactions as

$$\frac{d[FA]}{dt} = \frac{(V_{mDAG}[TAG][W] + V_{mMAG}[DAG][W] + V_{mG}[MAG][W])E_T}{([W] + K_{mDAG}[DAG] + K_{mMAG}[MAG] + K_{mG}[G])[FA]}$$

$$- \frac{(V_{rDAG}[DAG][FA] + V_{rMAG}[MAG][FA] + V_{rG}[G][FA])E_T}{([W] + K_{mDAG}[DAG] + K_{mMAG}[MAG] + K_{mG}[G])[FA]} \quad (19)$$

$$\frac{d[W]}{dt} = \frac{(V_{rDAG}[DAG][FA] + V_{rMAG}[MAG][FA] + V_{rG}[G][FA])E_T}{([W] + K_{mDAG}[DAG] + K_{mMAG}[MAG] + K_{mG}[G])[FA]}$$

$$- \frac{(V_{mDAG}[TAG][W] + V_{mMAG}[DAG][W] + V_{mG}[MAG][W])E_T}{([W] + K_{mDAG}[DAG] + K_{mMAG}[MAG] + K_{mG}[G])[FA]} \quad (20)$$

17

3. Parameters estimation

The concentrations change of each component with time could be obtained experimentally and the nonlinear curve fitting by Simplex's method was used for fitting the system of differential Eqs. (15) to (20) into the experimental data. Base upon the obtained rate constants and the kinetic scheme, the concentration of each composition at different reactions could be calculated. The concentration of each composition (triacylglycerol, diacylglycerol, monoacylglycerol and fatty acid) at different times was obtained experimentally when the substrate concentration of triacylglycerol and glycerol were 7.16 and 19.14 mM, respectively. The concentrations of enzyme and water were 600 mg and 9.89 mM, respectively. By fitting the above differential equations to the experimental data, the rate constants were calculated and listed in Table 2.

Table 2 Parameters in the model of glycerolysis reaction

Rate constants	Value
Initial maximum reaction rates (L/mg-h)	
V_{mDAG}	1.15×10^{-4}
V_{mMAG}	1.51×10^{-4}
V_{mG}	8.11×10^{-4}
V_{rDAG}	1.09×10^{-4}
V_{rMAG}	3.20×10^{-4}
V_{rG}	1.23×10^{-3}
Michaelis constants (mM^{-1})	
K_{mDAG}	1.09×10^{-4}
K_{mMAG}	3.20×10^{-4}
K_{mG}	1.23×10^{-3}

Comparison between calculated and experimental data was presented in Fig. 3 and a good agreement was obtained (the average difference between calculated and experimental data was less than 10^{-1} mM). Also calculated monoacylglycerol under various enzyme concentrations at constant concentrations of triacylglycerol (2.39 mM), glycerol (19.14 mM) and water (9.89 mM) were well agreed with the experimental data as shown in Fig. 4 (the average difference between calculated and experimental data was less than 10^{-1} mM). Therefore, the mechanism consecutive reversible hydrolysis and esterification reactions proposed in this study (Fig. 2) were adequate for glycerolysis of palm olein and glycerol.
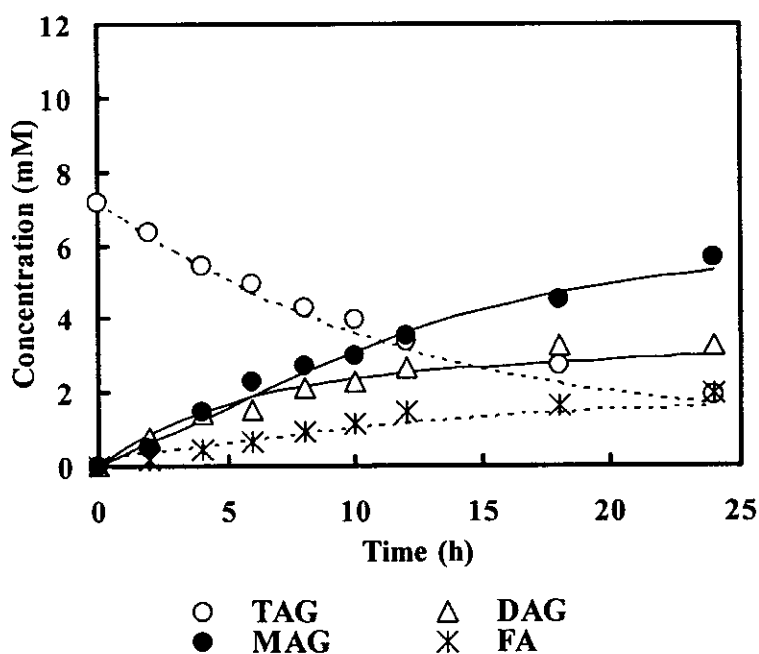
Figure 3 Comparison between calculated and experimental results (symbols) of glycerolysis reaction. Reaction condition: triacylglycerol 7.16 mM; glycerol 19.14 mM; water 9.89 mM; immobilized lipase 600 mg.
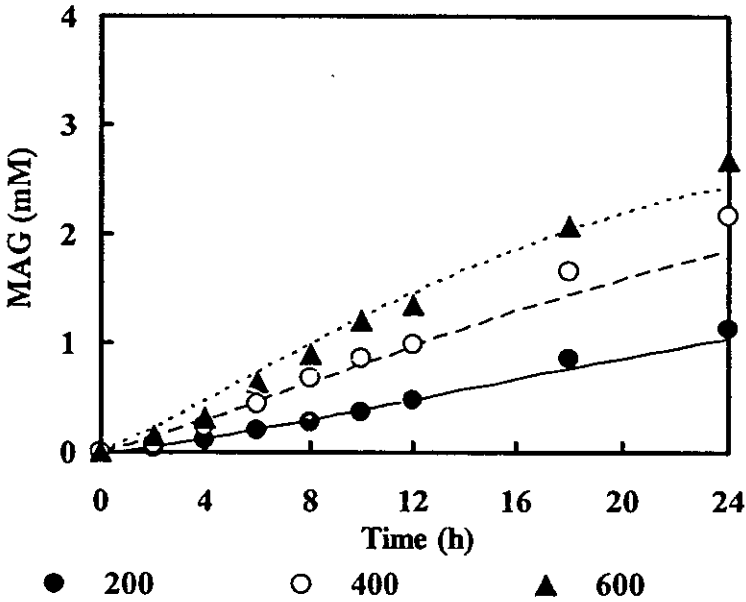
Figure 4 Comparison between calculated and experimental results (symbols) of monoacylglycerol production in glycerolysis reaction with various enzyme concentrations (200 to 600 mg).

In terms of the reaction rate constants in Table 2, the forward reaction rate constants in the first and second reactions ($V_{mDAG} = 1.15 \times 10^{-4}$ L/mg-h, $V_{mMAG} = 1.51 \times 10^{-4}$ L/mg-h) were much lower than that in the third forward reactions ($V_{mG} = 8.11 \times 10^{-4}$ L/mg-h). The results indicated that the first and second hydrolysis reactions (*TAG* to *DAG* and *DAG* to *MAG*) were the limit steps during the overall reactions. Because the reesterification reaction rate for *MAG* ($V_{rG} = 1.23 \times 10^{-3}$ L/mg-h) was higher than the hydrolysis reaction rate of *DAG* ($V_{mMAG} = 1.51 \times 10^{-4}$ L/mg-h), the intermediates (*G* and *FA* in *TAG* or *DAG*) were easily converted to *MAG*. The experimental results also showed that the concentration of the measurable intermediate (*FA*) was low during time course of glycerolysis (Fig. 3). For further study, the estimated parameters in Table 2 were used in the computer simulations to investigate the effect of each composition on glycerolysis reaction of palm olein.

4. Simulations of the effect of water concentration

The effect of changes in the value of the initial concentration of water (8 to 12% in glycerol) was investigated in a series of simulations in which the values of all other initial conditions were held constant (triacylglycerol 7.16 mM, glycerol 19.14 mM and enzyme concentration 600 mg). The simulation results were shown in Fig. 5.
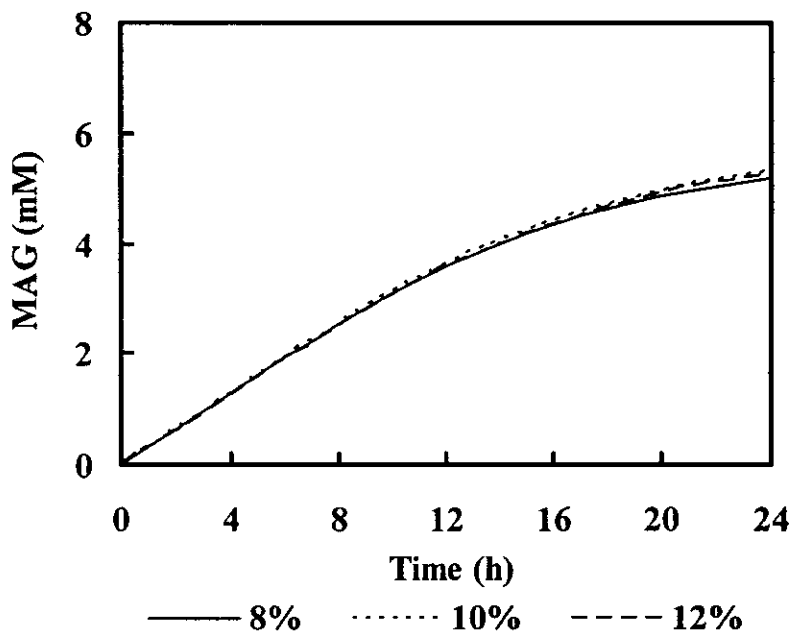

Figure 5 Simulation results of effect of water concentration (8 to 12% in glycerol) on the time dependence of monoacylglycerol.

The water concentration of 8% in glycerol was enough to enhance glycerolysis reaction. The initial concentration of water greater than 8% in glycerol, do not seem to increase more the initial production rate of monoacylglycerol. In addition, the total concentration of monoacylglycerol at equilibrium is relatively insensitive to water content.

5. Simulations of the effect of glycerol concentration

In this simulation, initial concentration of glycerol was varied in range of 10.74 to 21.49 mM while all other initial conditions (triacylglycerol 7.16 mM, water 9.89 mM and enzyme concentration 600 mg) were held constant. Figure 6 indicates that higher initial concentrations of glycerol lead to a faster initial rate of production of monoacylglycerol. In addition, the higher initial concentrations of glycerol result in greater extents of incorporation of glycerol into the fatty acid of palm olein (at equilibrium). This result shows that reesterification reaction of free fatty acid and glycerol precedes more than hydrolysis reaction of monoacylglycerol does in the present of high initial glycerol concentration. However, the concentration of glycerol higher than 19.14 mM resulted only slightly increasing in production rate and final concentration of monoacylglycerol.
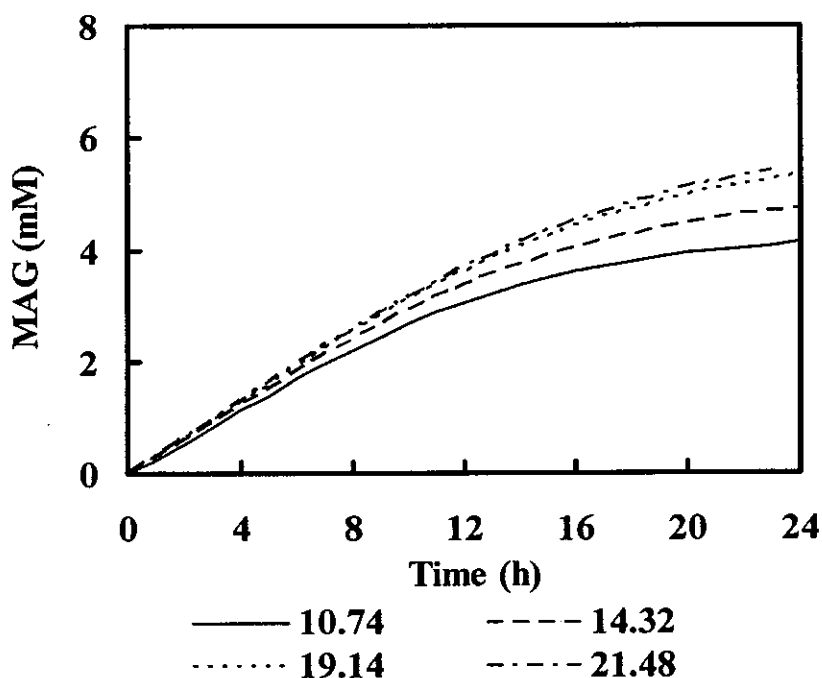

Figure 6 Simulation results of effect of glycerol concentration (10.74 to 21.48 mM) on the time dependence of monoacylglycerol.

6. Simulations of the effect of triacylglycerol concentration

In this simulation, initial concentration of palm olein was varied from 1.19 to 9.55 mM while holding initial concentrations of glycerol (19.14 mM), water (9.89 mM), and enzyme (600 mg) constant. Figure 7 depicts the resultant effects on the appearance of monoacylglycerol. The initial production rate of monoacylglycerol increases when the initial level of triacylglycerol increases. However, the production rate of monoacylglycerol near equilibrium point decreased when triacylglycerol increased.
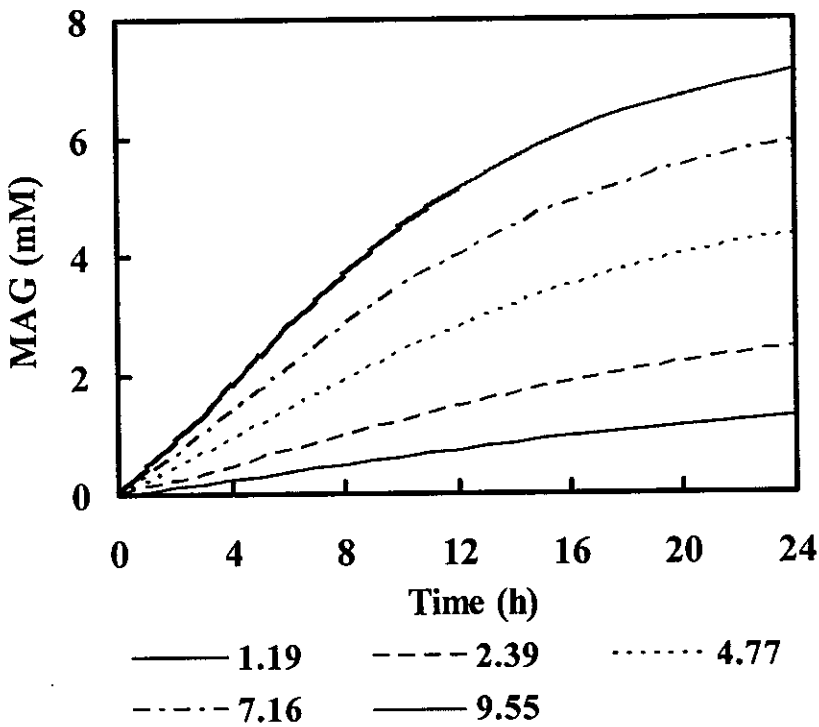

Figure 7 Simulation results of effect of palm olein concentration (1.19 to 9.55 mM) on the time dependence of monoacylglycerol.

7. Simulations of the effect of triacylglycerol and glycerol ratio

The effects of varying the initial concentrations of triacylglycerol and glycerol on the initial production rate and yield of monoacylglycerol were also simulated. Simulation of glycerolysis system under a variety of initial conditions provides a more complete picture of the dynamics and equilibrium behavior of this system (Fig. 8A and B).
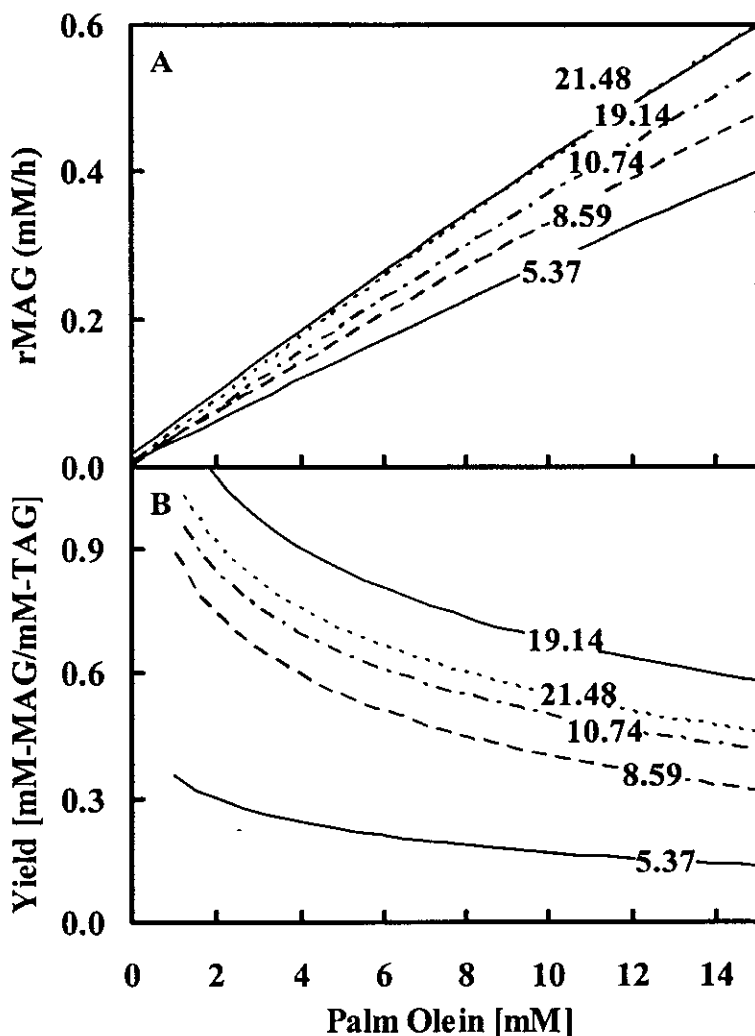

Figure 8 Simulation results of effects of palm olein concentration on the initial production rate (rMAG) and yield of monoacylglycerol at each glycerol concentration.

Two of the most significant findings were (1) an increase in the initial concentration of triacylglycerol leads to an increase in the initial production rate of monoacylglycerol, but there is a limit beyond which increasing the initial concentration of triacylglycerol results low yield of monoacylglycerol at each glycerol concentration and (2) increasing in glycerol concentration more than 19.14 mM the effect becomes less pronounced in initial production rate and yield of monoacylglycerol at equilibrium. The former result is expected from a thermodynamic standpoint, because a higher concentration of triacylglycerol should enhance the greater production rate of monoacylglycerol. The latter result might be due to the limitation of equilibrium comes from limited enzyme concentration. However, the production of monoacylglycerol increased with increasing enzyme concentration as shown in Fig. 4. Therefore, it was concluded that glycerol concentration of 19.14 mM was optimal concentration to enzyme concentration at 600 mg and at each triacylglycerol concentration.

8. Optimum conditions

From all of the above, it is clear that the proposed model equation can describe the glycerolysis reaction of palm olein at any substrate and glycerol concentrations. Then, it can be used to determine the optimal substrate and glycerol concentrations. In the case of high reaction rate and acceptable yield of monoacylglycerol were set as target in process optimization, the concentration of palm olein at 7.16 mM and glycerol at 19.14 mM were chosen to be carried out and experimental data were shown in Figure 9. The high production rate of monoacylglycerol of 0.338 mM h^{-1} and acceptable yield of 82% were obtained.
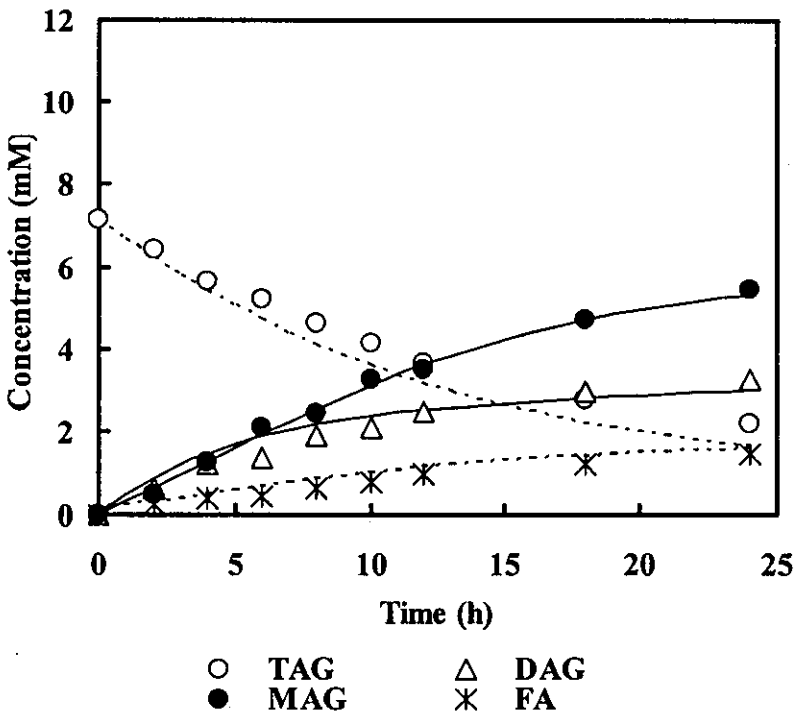
Figure 9   Comparison between calculated and experimental results (symbols) of glycerolysis reaction with the optimal initial production rate of monoacylglycerol.

On the other hand, in the case of high yield of monoacylglycerol was set as target in process optimization, low concentration of palm olein at 2.39 mM and excess of glycerol at19.14 mM were chosen and experimental data were shown in Figure 10. The highest yield of 100% was obtained. In both cases of the simulated and experimental data were in a good agreement.
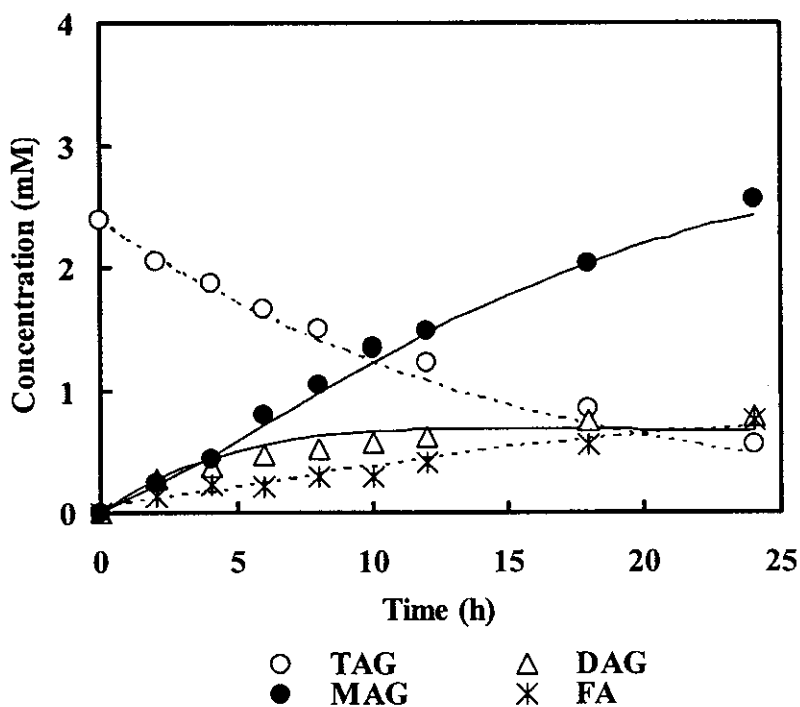

Figure 10 Comparison between calculated and experimental results (symbols) of glycerolysis reaction with the optimal yield of monoacylglycerol.

The constructed model summarized in Table 3 was useful to predict the behavior of immobilized lipase in glycerolysis reaction of palm oil. For further study, the model describing the process behavior can be used in fault diagnosis, performance estimation and prediction, scheduling, optimization and scale up.

Table 3 Summary of model for glycerolysis of palm oil by immobilized lipase

Reactant /Product	Model
TAG	$\dfrac{d[TAG]}{dt} = \dfrac{\left(-V_{mDAG}[TAG][W]+V_{rDAG}[DAG][FA]\right)E_T}{([W]+K_{mDAG}[DAG]+K_{mMAG}[MAG]+K_{mG}[G])[FA]}$
DAG	$\dfrac{d[DAG]}{dt} = \dfrac{\left(V_{mDAG}[TAG][W]+V_{rMAG}[MAG][FA]-V_{mMAG}[DAG][W]-V_{rDAG}[DAG][FA]\right)E_T}{([W]+K_{mDAG}[DAG]+K_{mMAG}[MAG]+K_{mG}[G])[FA]}$
MAG	$\dfrac{d[MAG]}{dt} = \dfrac{\left(V_{mMAG}[DAG][W]+V_{rG}[G][FA]-V_{mG}[MAG][W]-V_{rMAG}[MAG][FA]\right)E_T}{([W]+K_{mDAG}[DAG]+K_{mMAG}[MAG]+K_{mG}[G])[FA]}$
G	$\dfrac{d[G]}{dt} = \dfrac{\left(V_{mG}[MAG][W]-V_{rG}[G][FA]\right)E_T}{([W]+K_{mDAG}[DAG]+K_{mMAG}[MAG]+K_{mG}[G])[FA]}$
FA	$\dfrac{d[FA]}{dt} = \dfrac{\left(V_{mDAG}[TAG][W]+V_{mMAG}[DAG][W]+V_{mG}[MAG][W]\right)E_T}{([W]+K_{mDAG}[DAG]+K_{mMAG}[MAG]+K_{mG}[G])[FA]}$ $- \dfrac{\left(V_{rDAG}[DAG][FA]+V_{rMAG}[MAG][FA]+V_{rG}[G][FA]\right)E_T}{([W]+K_{mDAG}[DAG]+K_{mMAG}[MAG]+K_{mG}[G])[FA]}$
W	$\dfrac{d[W]}{dt} = \dfrac{\left(V_{rDAG}[DAG][FA]+V_{rMAG}[MAG][FA]+V_{rG}[G][FA]\right)E_T}{([W]+K_{mDAG}[DAG]+K_{mMAG}[MAG]+K_{mG}[G])[FA]}$ $- \dfrac{\left(V_{mDAG}[TAG][W]+V_{mMAG}[DAG][W]+V_{mG}[MAG][W]\right)E_T}{([W]+K_{mDAG}[DAG]+K_{mMAG}[MAG]+K_{mG}[G])[FA]}$